

# Formation of stimuli-responsive supramolecular polymeric assemblies *via* orthogonal metal–ligand and host–guest interactions†

Cite this: *Chem. Commun.*, 2013, **49**, 5951

Received 7th April 2013,  
Accepted 9th May 2013

DOI: 10.1039/c3cc42511h

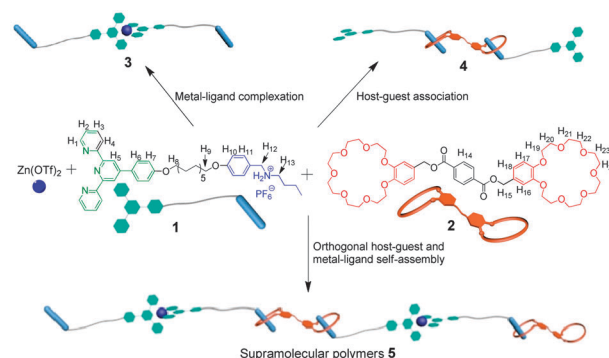
www.rsc.org/chemcomm

Yue Ding, Peng Wang, Yu-Kui Tian, Yu-Jing Tian and Feng Wang\*

**Linear supramolecular polymers, assembled *via* the combination of orthogonal terpyridine–Zn<sup>2+</sup> and benzo-21-crown-7/secondary ammonium salt recognition motifs, exhibit dynamic properties responsive to various external stimuli.**

The principle of orthogonal self-assembly, widely adopted by biological systems to demonstrate dedicated functionality in catalysis, recognition as well as signaling,<sup>1</sup> inspired the development of sophisticated artificial polymeric analogues.<sup>2</sup> As compared with conventional supramolecular polymers utilizing one type of non-covalent interaction, orthogonal self-assembly imparts much superior properties. First, simultaneous incorporation of multiple non-covalent bonds leads to a hierarchical assembly process with a high level of complexity. Second, considering each type of non-covalent interaction is inherently reversible, manipulating non-covalent bonds separately addresses adaptive properties of the resulting supramolecular assemblies.<sup>3</sup> Up to now, a variety of self-assembling architectures, such as supramolecular block copolymers,<sup>4</sup> graft copolymers,<sup>5</sup> networks<sup>6</sup> and single-chain nanoparticles,<sup>7</sup> have been fabricated using the orthogonal self-assembling approach.

We endeavor to explore novel types of orthogonal building blocks, and furthermore develop them into highly adaptive supramolecular polymeric assemblies. Crown ether based host–guest interaction, derived from the threading property, renders unusual mobility and unique mechanical behavior to the resulting rotaxane-type interlocked structures.<sup>8</sup> Meanwhile, coordination of 2,2':6',2''-terpyridine (tpy) to a wide range of transition metal ions provides an ideal platform to combine high thermodynamic stability with tunable kinetics.<sup>9</sup> Therefore, our strategy involves the integration of these two non-covalent interactions. Specifically, heteroditopic monomer **1** is designed which bears a secondary ammonium salt guest and a terpyridine ligand on each side (Scheme 1). Upon addition of Zn(OTf)<sub>2</sub>, it is expected to form a 2:1 terpyridine–Zn<sup>2+</sup>



**Scheme 1** Schematic representation of the formation of supramolecular polymers **5** and the corresponding intermediates (terpyridine–Zn<sup>2+</sup> dimeric complex **3** and host–guest paired [3]pseudorotaxane structure **4**).

complex **3**. In addition, **1** could also associate with the complementary homoditopic benzo-21-crown-7 (B21C7) monomer **2** to achieve [3]pseudorotaxane structure **4**. If terpyridine–metal and B21C7/secondary ammonium salt recognition motifs are proved to be completely orthogonal, mixing three components (monomers **1–2**, Zn(OTf)<sub>2</sub>) in a specific ratio would guarantee the formation of linear supramolecular polymers **5** with stimuli-responsive and adaptive behaviors.

The synthetic routes to the desired monomers **1–2** are quite straightforward (Schemes S1 and S2, ESI†). It is worthy of note that the length mismatch of monomers **1–2**, accomplished *via* introducing a flexible aliphatic spacer on monomer **1**, would destabilize the cyclic oligomers and thereby favor the linear extension,<sup>10</sup> resulting in a relatively low critical polymerization concentration (CPC) for the supramolecular polymerization process.

Slow-exchange host–guest complexation between compounds **1** and **2** was elucidated using the <sup>1</sup>H NMR spectrum (Fig. S8, ESI†), which exhibits three sets of signals for the protons belonging to the B21C7/secondary ammonium salt recognition motif.<sup>8a</sup> For the resulting host–guest paired dimer **4**, aromatic protons H<sub>10–11</sub> and methylene protons H<sub>12</sub> on **1**, as well as ethyleneoxy protons H<sub>19–20</sub> on **2**, move downfield significantly, supporting the formation of [3]pseudorotaxane structure. On the other hand, no obvious chemical shift change occurs for the terpyridine unit, demonstrating

Key Laboratory of Soft Matter Chemistry, Department of Polymer Science and Engineering, University of Science and Technology of China, Hefei, Anhui 230026, P.R. China. E-mail: drfwang@ustc.edu.cn; Fax: +86551 6360 6095

† Electronic supplementary information (ESI) available: Synthesis, characterization, UV-Vis titration data and other materials. See DOI: 10.1039/c3cc42511h

the preferential host-guest complexation without the involvement of the terpyridine ligand.

Next, the capability to form  $\text{Zn}^{2+}$ -terpyridine complexes was investigated by UV/Vis measurements. Stepwise titration of  $\text{Zn}(\text{OTf})_2$  with monomer **1** shows a clear isosbestic point at 315 nm (Fig. S9, ESI<sup>†</sup>), indicating the efficient conversion from free to metal-complexed terpyridine species. The achievement of maximum absorbance ( $\lambda_{\text{max}} = 343$  nm) at the  $\text{Zn}(\text{OTf})_2/\mathbf{1}$  molar ratio of 0.5 apparently supports the formation of a 2 : 1 complex for terpyridine and  $\text{Zn}^{2+}$ . After validating the two-component model systems, we turned to examining metal-ligand complexation in the presence of host-guest counterparts. Therefore, a 2 : 1 mixture of monomers **1** and **2** was titrated with  $\text{Zn}(\text{OTf})_2$  in the manner described above (Fig. S10, ESI<sup>†</sup>). The resulting titration curves, resembling the plots depicted in Fig. S9 (ESI<sup>†</sup>), exhibit a similar linear increase and a sharp endpoint at a  $\text{Zn}^{2+}$ /terpyridine ratio of 0.5 : 1 (Fig. 1a), illustrating the specific complexation between  $\text{Zn}^{2+}$  and terpyridine without the participation of host-guest units.

It should be noted that UV/Vis experiments could not distinctly distinguish various types of metal-ligand complexes such as  $\text{Zn}(\text{tpy})_2^{2+}$  and  $\text{Zn}(\text{tpy})_2^{2+}$ . Therefore, deeper insights into the exchange kinetics of  $\text{Zn}^{2+}$ -terpyridine complexes were provided by  $^1\text{H}$  NMR titration measurements, by means of titration of  $\text{Zn}(\text{OTf})_2$  with a 2 : 1 mixture of monomers **1** and **2**. When the feed ratio of  $\text{Zn}^{2+}/\text{tpy}$  is below 0.5 (Fig. 2a–c), the complexed terpyridine proton  $\text{H}_5$  shifts downfield, while  $\text{H}_1$  reveals a remarkable upfield shift from 8.74 to 7.80 ppm, mainly attributing to the shielding effect of the neighboring terpyridine unit. Once an exact 1 : 2  $\text{Zn}^{2+}$ -terpyridine molar ratio is achieved (Fig. 2c), original uncomplexed signals totally disappear, representing the formation of dimeric  $\text{Zn}(\text{tpy})_2^{2+}$  structure **3**. However, once the  $\text{Zn}^{2+}$ /terpyridine ratio is further increased to 3 : 2, a third set of signals evolve and gradually strengthen, along with the disappearance of  $\text{Zn}(\text{tpy})_2^{2+}$  signals (Fig. 2e), suggesting the formation of a 1 : 1 metal-ligand complex  $\text{Zn}(\text{tpy})_2^{2+}$  with the additional coordination sites saturated by solvent or triflate counterions.<sup>11</sup> Kinetically labile property of the  $\text{Zn}^{2+}$ -terpyridine complex is also observed for the model system containing monomer **2** and  $\text{Zn}(\text{OTf})_2$  without the presence of homoditopic host **1** (Fig. S11, ESI<sup>†</sup>), which further demonstrates that terpyridine- $\text{Zn}^{2+}$  complexation is not interfered by the neighboring B21C7/secondary ammonium salt recognition motif.

After confirming orthogonal self-assembling properties of terpyridine- $\text{Zn}^{2+}$  and B21C7/secondary ammonium salt recognition motifs, concentration-dependent  $^1\text{H}$  NMR measurements were

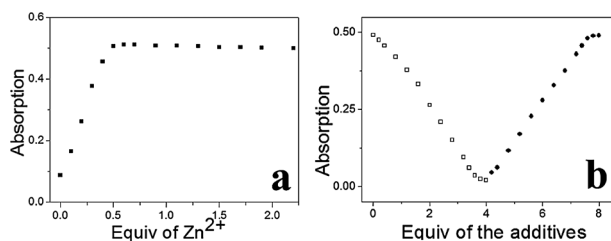


**Fig. 1** Development of a UV/Vis absorbance band at 343 nm in  $\text{CHCl}_3\text{-CH}_3\text{CN}$  (3/1, v/v). (a) Titration of a 2 : 1 mixture of monomers **1** and **2** (0.02 mM and 0.01 mM, respectively) with  $\text{Zn}(\text{OTf})_2$ ; (b) stepwise addition of a competitive ligand cyclen ( $\square$ ) and  $\text{Zn}(\text{OTf})_2$  ( $\bullet$ ) to a 1 : 2 : 1 mixture of  $\text{Zn}(\text{OTf})_2$ , **1** and **2**.

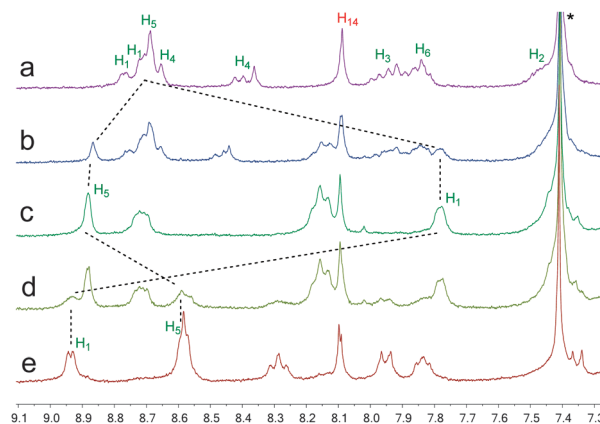


**Fig. 2**  $^1\text{H}$  NMR titration (300 MHz,  $\text{CDCl}_3\text{-CD}_3\text{CN}$  (3/1, v/v), 25 °C) of 2 : 1 mixtures of monomers **1** and **2** (4 mM and 2 mM, respectively) with increasing equivalents of  $\text{Zn}(\text{OTf})_2$ : (a) 0 equiv.; (b) 0.2 equiv.; (c) 0.5 equiv.; (d) 0.8 equiv.; (e) 1.5 equiv. of  $\text{Zn}(\text{OTf})_2$  versus the terpyridine unit.

performed to evaluate the monomer concentration effect on the formation of linear supramolecular polymers **5** (Fig. S12, ESI<sup>†</sup>). Upon mixing a 1 : 2 : 1 molar ratio of  $\text{Zn}(\text{OTf})_2$ , **1** and **2** in  $\text{CDCl}_3\text{-CD}_3\text{CN}$  (3/1, v/v) at low concentration, well-defined signals for B21C7/secondary ammonium salt moieties in  $^1\text{H}$  NMR spectra indicate the domination of cyclic oligomers. As the monomer concentration gradually increases, the original cyclic benzylic protons  $\text{H}_{15}$  and ethyleneoxy protons of the B21C7 unit progressively decrease, whilst the newly formed linear species gradually strengthen, revealing the formation of high-molecular-weight aggregates at high concentration. On the other hand, free terpyridine units are completely converted to metal-complexed states for all the measured concentrations, consistent with UV/Vis titration results. Moreover, their signals remain almost unchanged between cyclic oligomers and linear supramolecular polymers, presumably due to the similar chemical environment for these two species.

Subsequently, two-dimensional diffusion-ordered NMR (DOSY) experiments were also performed. As the monomer concentration increased from 4.00 mM to 80.0 mM, the measured diffusion coefficients decrease considerably from  $3.57 \times 10^{-10}$  to  $6.37 \times 10^{-11} \text{ m}^2 \text{ s}^{-1}$  (Fig. S13, ESI<sup>†</sup>). The result, in line with the above concentration-dependent  $^1\text{H}$  NMR result, suggests that monomer concentration exerts a significant impact on the reversible supramolecular polymerization process.

Macroscopic properties of the resulting supramolecular assemblies were further investigated by capillary viscosity measurements. All of the experiments were performed in  $\text{CHCl}_3\text{-CH}_3\text{CN}$  (3/1, v/v) containing 0.05 M tetrabutylammonium hexafluorophosphate to exclude the polyelectrolyte effect. Specific viscosities of the dimeric  $\text{Zn}(\text{tpy})_2^{2+}$  complex **3**, as well as host-guest paired dimer **4**, give comparably shallow curves (Fig. 3a). In sharp contrast, the specific viscosity of a 1 : 2 : 1 mixture of  $\text{Zn}(\text{OTf})_2$ , **1** and **2** changes exponentially as a function of monomer concentration, characteristic of the formation of high-molecular-weight polymers **5**. Such phenomena clearly support that both of the orthogonal metal-ligand and host-guest self-assembling motifs are indispensable for the chain extension. Attributing to the length mismatch effect of the two monomers, the propensity to form cyclic species is efficiently suppressed, as reflected by the relatively low CPC value (9 mM, Fig. S14, ESI<sup>†</sup>).

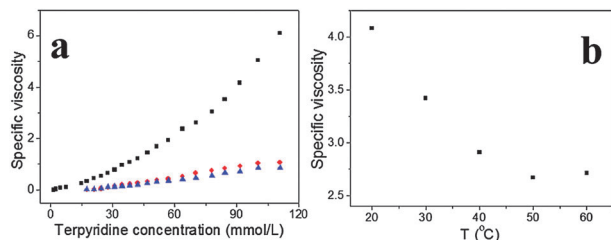


**Fig. 3** (a) Specific viscosities of the linear supramolecular polymers **5** (■), dimeric  $\text{Zn}(\text{tpy})_2^{2+}$  complex **3** (●), and host-guest paired [3]pseudorotaxane **4** (▲) ( $\text{CHCl}_3\text{--CH}_3\text{CN}$  (3/1, v/v), 293 K) as a function of terpyridine unit concentration; (b) temperature-dependent specific viscosity of **5** at terpyridine unit concentration of 90 mM.

Dynamic properties of the resulting supramolecular polymers **5** were further evaluated with a variety of external stimuli. Specific viscosity of the supramolecular polymers **5** reduces significantly above 50 °C, indicating the disassembly of supramolecular polymers at elevated temperature (Fig. 3b). Detailed  $^1\text{H}$  NMR measurement reveals that host-guest interactions are more susceptible to the temperature variation (Fig. 4a). Moreover, adding 1.5 equiv. of  $\text{Et}_3\text{N}$  deprotonates the secondary ammonium salt units, leading to the considerable reduction of characteristic [3]pseudorotaxane signals and thereby breaking up the supramolecular polymers **5** (Fig. 4c). Subsequent addition of 2.8 equiv. of  $\text{CF}_3\text{COOH}$  could almost restore the polymeric assemblies (Fig. 4d), as reflected by the enhancement of complexed benzylic protons  $\text{H}_{15}$  in the  $^1\text{H}$  NMR spectrum.<sup>12</sup>

On the other hand, metal-ligand interaction could also be manipulated *via* the addition of a stronger  $\text{Zn}^{2+}$ -chelating agent, 1,4,7,10-tetraazacyclododecane (cyclen).<sup>13</sup> Specifically, adding 4 equiv. of cyclen results in the total disappearance of  $\text{Zn}^{2+}/\text{tpy}$  absorption bands ( $\lambda_{\text{max}} = 343$  nm). Furthermore, reformation of supramolecular polymers **5** could be achieved *via* the addition of equal amounts of  $\text{Zn}(\text{OTf})_2$ , as verified by the reappearance of the  $\text{Zn}^{2+}/\text{tpy}$  absorption band (Fig. 1b and Fig. S15, ESI†). Hence, it is evident that supramolecular polymers **5** are highly adaptive, capable of undergoing reversible transitions under a variety of external stimuli.

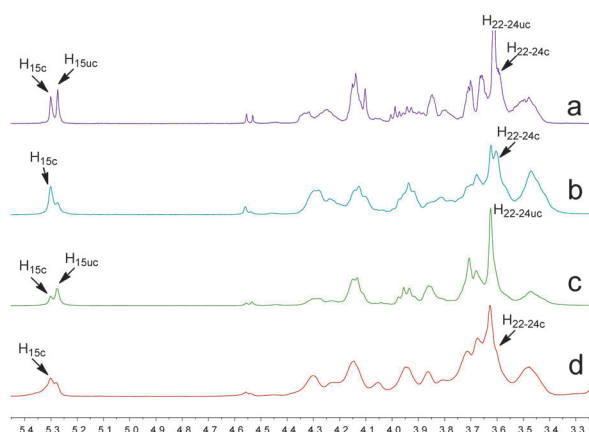


**Fig. 4** Partial  $^1\text{H}$  NMR spectra (300 MHz,  $\text{CDCl}_3\text{--CD}_3\text{CN}$  (3/1, v/v)) of a 1:2:1 mixture of  $\text{Zn}(\text{OTf})_2$ , **1** and **2** at terpyridine unit concentration of 36 mM: (a) 60 °C; (b) 25 °C; (c) treating the mixture with 1.5 equiv. of  $\text{Et}_3\text{N}$  at 25 °C; (d) subsequent addition of 2.8 equiv. of  $\text{CF}_3\text{COOH}$ .

In conclusion, we demonstrated that terpyridine- $\text{Zn}^{2+}$  and B21C7/secondary ammonium salt motifs recognize each other in an orthogonal manner. Novel linear supramolecular polymers **5** could be successfully constructed *via* the combination of these two non-covalent recognition motifs, which were confirmed by  $^1\text{H}$  NMR, UV/Vis, DOSY and viscosity measurements. The resulting supramolecular polymers exhibit multi-stimuli responsiveness capabilities, as triggered by heat, pH or a competitive ligand, cyclen. Such adaptive assemblies would be an appealing choice for further fabrication of intelligent supramolecular materials with tailored properties.

This work was supported by the National Natural Science Foundation of China (21274139, 91227119), the Fundamental Research Funds for the Central Universities, and the Anhui Provincial Natural Science Foundation.

## Notes and references

- M. Garcia-Viloca, J. Gao, M. Karplus and D. G. Truhlar, *Science*, 2004, **303**, 186.
- (a) S. A. Levi, P. Guatteri, F. C. J. M. van Veggel, G. J. Vancso, E. Dalkanale and D. N. Reinhoudt, *Angew. Chem., Int. Ed.*, 2001, **40**, 1892; (b) S.-L. Li, T. Xiao, C. Lin and L. Wang, *Chem. Soc. Rev.*, 2012, **41**, 5950; (c) L. J. Marshall and J. de Mendoza, *Org. Lett.*, 2013, **15**, 1548; (d) C.-H. Wong and S. C. Zimmerman, *Chem. Commun.*, 2013, **49**, 1679.
- (a) B. Rybtchinski, *ACS Nano*, 2011, **5**, 6791; (b) X. Yan, F. Wang, B. Zheng and F. Huang, *Chem. Soc. Rev.*, 2012, **41**, 6042.
- (a) H. Hofmeier, R. Hoogenboom, M. E. L. Wouters and U. S. Schubert, *J. Am. Chem. Soc.*, 2005, **127**, 2913; (b) F. Wang, C. Han, C. He, Q. Zhou, J. Zhang, C. Wang, N. Li and F. Huang, *J. Am. Chem. Soc.*, 2008, **130**, 11254; (c) S. K. Yang, A. V. Ambade and M. Weck, *J. Am. Chem. Soc.*, 2010, **132**, 1637; (d) Y. Liu, Y. Yu, J. Gao, Z. Wang and X. Zhang, *Angew. Chem., Int. Ed.*, 2010, **49**, 6576; (e) F. Grimm, N. Ulm, F. Groehn, J. Duering and A. Hirsch, *Chem.-Eur. J.*, 2011, **17**, 9478; (f) S.-L. Li, T. Xiao, Y. Wu, J. Jiang and L. Wang, *Chem. Commun.*, 2011, **47**, 6903; (g) G. Groeger, W. Meyer-Zaika, C. Boettcher, F. Groehn, C. Ruthard and C. Schmuck, *J. Am. Chem. Soc.*, 2011, **133**, 8961; (h) Z. Zhang, Y. Luo, J. Chen, S. Dong, Y. Yu, Z. Ma and F. Huang, *Angew. Chem., Int. Ed.*, 2011, **50**, 1397.
- K. P. Nair and M. Weck, *Macromolecules*, 2007, **40**, 211.
- (a) F. Wang, J. Zhang, X. Ding, S. Dong, M. Liu, B. Zheng, S. Li, L. Wu, Y. Yu, H. W. Gibson and F. Huang, *Angew. Chem., Int. Ed.*, 2010, **49**, 1090; (b) P. Du, J. Liu, G. Chen and M. Jiang, *Langmuir*, 2011, **27**, 9602; (c) Y.-K. Tian, L. Chen, Y.-J. Tian, X.-Y. Wang and F. Wang, *Polym. Chem.*, 2013, **4**, 453.
- N. Hosono, M. A. J. Gillissen, Y. Li, S. S. Sheiko, A. R. A. Palmans and E. W. Meijer, *J. Am. Chem. Soc.*, 2013, **135**, 501.
- (a) C. Zhang, S. Li, J. Zhang, K. Zhu, N. Li and F. Huang, *Org. Lett.*, 2007, **9**, 5553; (b) S. Dong, Y. Luo, X. Yan, B. Zheng, X. Ding, Y. Yu, Z. Ma, Q. Zhao and F. Huang, *Angew. Chem., Int. Ed.*, 2011, **50**, 1905; (c) Z. Niu, F. Huang and H. W. Gibson, *J. Am. Chem. Soc.*, 2011, **133**, 2836; (d) B. Zheng, F. Wang, S. Dong and F. Huang, *Chem. Soc. Rev.*, 2012, **41**, 1621.
- (a) W. C. Yount, D. M. Loveless and S. L. Craig, *Angew. Chem., Int. Ed.*, 2005, **44**, 2746; (b) W. C. Yount, D. M. Loveless and S. L. Craig, *J. Am. Chem. Soc.*, 2005, **127**, 14488; (c) M. Burnworth, L. Tang, J. R. Kumpfer, A. J. Duncan, F. L. Beyer, G. L. Fiore, S. J. Rowan and C. Weder, *Nature*, 2011, **472**, 334; (d) G. Du, E. Moulin, N. Jouault, E. Buhler and N. Giuseppone, *Angew. Chem., Int. Ed.*, 2012, **51**, 12504.
- N. Yamaguchi and H. W. Gibson, *Chem. Commun.*, 1999, 789.
- R. Dobrawa, M. Lysetska, P. Ballester, M. Gruene and F. Wurthner, *Macromolecules*, 2005, **38**, 1315.
- L. Chen, Y.-K. Tian, Y. Ding, Y.-J. Tian and F. Wang, *Macromolecules*, 2012, **45**, 8412.
- B. Gruber, E. Kataev, J. Aschenbrenner, S. Stadlbauer and B. Koenig, *J. Am. Chem. Soc.*, 2011, **133**, 20704.